ELSEVIER

Biochimica et Biophysica Acta 1479 (2000) 275–285

BIOCHIMICA ET BIOPHYSICA ACTA
BBA

www.elsevier.com/locate/bba

Conformational study of a custom antibacterial peptide cecropin B1: implications of the lytic activity

S. Srisailam [a], A. I. Arunkumar [a], W. Wang [b], C. Yu [a,*], H. M. Chen [b,1]

[a] *Department of Chemistry, National Tsing Hua University, Hsinchu, Taiwan*
[b] *Department of Biochemistry, Hong Kong University of Science and Technology, Hong Kong, China*

Received 13 July 1999; received in revised form 13 October 1999; accepted 19 January 2000

Abstract

Cecropin B1 (CB1) with two amphipathic α-helical segments is a derivative of the natural antibacterial peptide, cecropin B. The assays of cell lysis show that, compared with cecropin A (CA), CB1 has a similar ability to lyse bacteria with a higher potency (two- to six-fold higher) in killing cancer cells. The difference may be due to the fact that the peptides possess different structures and sequences. In this study, the solution structure of CB1 in 20% hexafluoroisopropanol was determined by two-dimensional nuclear magnetic resonance (NMR) spectroscopy. The ^{1}H NMR resonances were assigned. A total of 350 inter-proton distances were used to calculate the solution structure of CB1. The final ensemble structures were well converged, showing the minimum root mean square deviation. The results indicate that CB1 has two stretches of helices spanning from residues 3 to 22 and from residues 26 to 33, which are connected by a hinge section formed by Gly-23 and Pro-24. Lys-25 is partially incorporated in the hinge region. The bent angle between two helical segments located in two planes was between 100 and 110°. With comparisons of the known NMR structure of CA and its activities on bacteria and cancer cells, the structure–function relationship of the peptides is discussed.

Keywords: Nuclear magnetic resonance; Conformation; Cecropin; Lysis

1. Introduction

Natural antibacterial peptides are widely found in the animal kingdom. These peptides are highly potent in lysing bacteria. Usage of these peptide antibiotics may be gradually appreciated since more bacteria may develop the ability to resist conventional antibiotics due to the abuse of these drugs worldwide [1]. Many antibacterial peptides have been found to have impressive in vitro [2–4] and in vivo [5] activities to kill cancer cells without damaging the normal eukaryotic cells. A recent report [6] further indicated that expressions of the antimicrobial peptides such as cecropin and melittin in human cells were found to have anti-tumor properties. However, the mechanism by which the peptides kill both prokaryotic and transformed eukaryotic cells is not well understood. It is believed that the amount of secondary structure formed as they approach the cell membrane and the content of the cationic residues in sequence [7–9] may play an important role in the lysis of cell membranes. However, it is not clear whether the structure or the

Abbreviations: CA, cecropin A; CB, cecropin B; CB1, cecropin B1; CB3, cecropin B3; HFP, 1,1,1,3,3,3-hexafluoro-2-propanol; IC_{50}, inhibitory concentration at which the cell viability is 50%; LC, lethal concentration; RMSD, root mean square deviation

* Corresponding author. E-mail: cyu@mx.nthu.edu.tw
[1] Also corresponding author. E-mail: bchmc@ust.hk

0167-4838/00/$ – see front matter
PII: S0167-4838(00)00008-X

sequence plays a dominant role in lysing the cell membranes. From a structural point of view, these peptide antibiotics [10] form diversified structures such as α-helices (cecropins, magainins and melittins), β-strands (defensins, thionins, tachyplesins and protegrins), extended coils (indolicidin and bac 5) or loops (bactencin and gramicidin S) upon approaching cell membranes, which initiate the action of cell lysis. The different binding mode and interaction profiles in various cell membranes may cause peptides to form specific conformations. The structure–function relationship of the peptides with various conformations remains to be elucidated.

Cecropins are a family of peptide antibiotics [11] which are widely found in the immune hemolymph of silk moth and mammals [12,13]. They are composed of 34–39 amino acids and have high sequence homology. The primary sequences of naturally occurring cecropins have an N-terminal segment mostly made up of basic residues contributing to the amphipathic helix and a C-terminal segment basically composed of hydrophobic residues. Solution structures of cecropin A (CA), a hybrid peptide of cecropin A and melittin (CAM), and cecropin P1 (CP1) have been determined. Two-dimensional nuclear magnetic resonance (2D NMR) techniques were used to investigate the solution structure of CA in 15% (v/v) hexafluoroisopropanol (HFP) at pH 5.0 [14]. Analysis of 21 converged structures showed that two helical segments extending from residues 5 to 21 and from residues 24 to 37 were identified. These two helices located in two planes have a bent angle between 70 and 100°. The orientation of the helices within these planes was not determined. CAM was found to have a higher bacteria killing ability with a broader spectrum than either CA or melittin, and has no effect on the lysis of mammalian cells [15]. The structure of CAM was also investigated by 2D ^{1}H NMR in 30% HFP at pH 5 [16]. All proton resonances were assigned except for the first residue, Lys. Results showed that CAM has both an N-terminal (residues 4–12) and a C-terminal α-helix (residues 16–26). The C-terminal α-helical segment was found to be more stable than the N-terminal one. It was concluded that a typical structure with a hydrophobic α-helix and an amphiphilic α-helix connected by a flexible hinge section in between is an important feature for a peptide to perform lytic activity on cell membranes. The NMR structure of CP1 isolated from pig intestine [17] was further studied by the same group [18] in 30% (v/v) HFP and pH 5.0. Similar to CAM, all proton resonances were assigned for CP1 except the first residue, Ser. It was intriguing that the structure of CP1 was different from the helix-hinge-helix structure found in either CA or CAM. A single and long α-helical structure of CP1 with an amphipathic section of 4–5 turns and a short hydrophobic section of 1–2 turns was identified. The results showed that CP1 could easily span through lipid bilayers. Recently, a multi-point mutation of Abp3, an analog of cecropin B, was found to display higher bacteriolytic activity than cecropin B and its solution structure has been determined by 2D NMR [19]. All the above peptides, CA, CAM, CP1 and Abp3, have a common motif of helix-hinge-helix (except CP1 with a continuous α-helix) and possess cell killing ability with different degrees and specificities.

In this communication, we investigated the solution NMR structure of the custom peptide, cecropin B1 (CB1), with two amphipathic α-helical segments derived from natural cecropin B (CB) (for peptide sequences, see Section 2). The experiments were done at the optimum conditions and the results were compared with known data of CA [14]. In addition to the structure, we further conducted cytotoxicity assays on leukemia cells using these two peptides. The relationship between structure and function can therefore be explored. In correlation with our previous report on lethal concentrations of CB1 and CA on bacteria [2], the differences between the peptides in structure and potency on cell membranes are discussed.

2. Materials and methods

2.1. Materials

The RPMI 1640 medium, 1,1,1,3,3,3-hexafluoro-2-propanol (HFP), hydrochloric acid, sodium bicarbonate, and sodium hydroxide used in this experiment were purchased from Sigma, USA. Cell culture media like F-12 nutrient mixture (Ham), fetal bovine serum (FBS) and Dulbecco's modified Eagle's medium (D-MEM) were obtained from Gibco, USA. Micorotetrazolium assay kit was purchased from

Boehringer Mannheim, Germany. The leukemia cell lines like HL-60, K-562, Jurkat (E6-1) and CCRF-CEM and fibroblast cell 3T6 were ordered from American Type Culture Collection (ATCC), USA. Sodium 3-(trimethyl silyl) [2,2,3,3,-^{2}H] propionate (d_4-TSP) (99.5% purity), deuterated water (D_2O) (99.9% purity) and deuterated hexafluoroisopropanol (d_2-HFP; 98% purity) were obtained from Cambridge Isotope Laboratory, USA. The water used in this study was deionized from Milli-Q water purification system (Millipore, USA).

2.2. Peptide synthesis

Synthesis of peptides CA and CB1 was carried out as previously reported [2,20]. Both amino acid composition and molecular weight were determined by mass spectrometry. Results indicated that total number of amino acids and molecular weights are: 37/4004 for CA, and 34/4113 for CB1. These data agree well with the peptide primary sequences. The peptide solution was lyophilized after purification (for details, see [2]). A microbalance (Sartorius Research Model R200D; ±0.01 mg) was used to measure the weight of dried products. Peptide concentrations were determined from their dry weight. Amino acid sequences of CA, CB and CB1 are as follows: CA: (NH_2)-KWKLFKKIEKVGQNIRDGIIKAGPAVAVVGQATQIAK-($CONH_2$); CB: (NH_2)-KWKVFKKIEKMGRNIRNGIVKAGPAIAVLGEAKAL-($CONH_2$); CB1: (NH_2)-KWKVFKKIEKMGRNIRNGIVKAGPKWKVFKKIEK-($CONH_2$).

In CA, the first underlined segment is the amphipathic helix and the second segment is the hydrophobic helix [14]. CB1 was designed by replacing the last 11 residues of CB by the segment from positions 1 to 10 of CB (underlined in CB).

2.3. Sample preparations

2.3.1. Cell culture and cytotoxicity assay

The IC_{50} values of CA and CB1 on typical leukemia cells such as HL-60, K-562, Jurkat (E6-1) and CCRF-CEM were measured. Fresh venous blood was stored in an EDTA bottle. The pellet of erythrocytes was washed with D-PBS buffer four times. The detailed procedures of cell culturing and the assay of cell lysis have been shown elsewhere [2,21].

2.3.2. Preparation of NMR sample

NMR sample was prepared to a final concentration of 2 mM by dissolving 4 mg of CB1 in a mixture containing 80% (v/v) H_2O and 20% (v/v) d_2-HFP. The pH of the solution was adjusted to 4.2. d_4-TSP was used as an internal standard.

2.4. NMR spectroscopy

All NMR measurements were carried out on a 600 MHz Bruker DMX-600 spectrometer. A 2D TOCSY of 70 ms mixing time [22,23] and a NOESY of 200 ms were recorded at 20°C and 32°C. In the TOCSY experiment, the numbers of data points in t_1 and t_2 were 512 and 2048, respectively, and each increment was the sum of 64 scans of FIDs. In the NOESY experiment, a total of 88 scans were accumulated for each increment of t_1 and the spectra were recorded using TPPI phase sensitive mode under the situation of pre-saturation during relaxation delay and mixing time [24].

2.5. Structure calculation

All energy minimization and dynamical simulated annealing calculations were carried out according to Nilges et al. [25,26] on an INDY workstation using X-PLOR software [27,28]. The calculations were based on the distance constraints obtained from NOEs pooled from a 200 ms NOESY spectrum. The structure calculation was initiated with 50 random structures followed by the dynamical simulated annealing protocol [25,26]. A total of 12 final structures were chosen based on the minimum NOE violation and the lowest conformational energy. The structures were overlapped and displayed using QUANTA software (see Fig. 6).

3. Results and discussion

3.1. Anticancer activities of CA and CB1

Both CA and CB1 can inhibit almost all kinds of leukemia cells. The IC_{50} values (μM) of CA and CB1 on some typical leukemia cells are shown in Table 1. These peptides do not affect healthy vertebrate cells at these concentrations. For comparison, the IC_{50}

Table 1
Measurements of the IC_{50} values of CA and CB1 on leukemia cells and the lethal concentration (LC) of CA and CB1 on Gram-negative bacteria

Cell line	IC_{50}^{b} (CA)	IC_{50} (CB1)	Bacteria	LC[a] (CA)	LC[a] (CB1)
HL-60	22.0 ± 1.4	7.5 ± 0.5	*Klebsiella pneumoniae*	0.33 ± 0.021	0.39 ± 0.015
K-562	20.0 ± 1.1	10.2 ± 0.7	*Escherichia coli*	0.45 ± 0.022	0.49 ± 0.002
Jurkat (E6-1)	15.8 ± 0.9	2.4 ± 0.3	*Pseudomonas aeruginosa*	1.43 ± 0.004	1.48 ± 0.021
CCRF-CEM	17.8 ± 1.1	8.6 ± 0.5			
3T6 (fibroblast cells)	> 50	> 50			
Erythrocytes	> 100 (HE_{50}^{c})	> 100 (HE_{50})			

The results are the average of at least three experiments and the average deviations are shown. The unit used for the IC_{50} and the LC is μM.
[a]The data were obtained from our previous report (see [2]).
[b]The IC_{50} is the concentration of peptide (CA or CB1) at which cell viability is 50%.
[c]The HE_{50} is the concentration of peptide (CA or CB1) at which hemolysis is 50%.

values of CA/CB1 on healthy vertebrate cells such as fibroblast cells (3T6) and erythrocytes are also shown in Table 1. It is known that cecropins can kill most Gram-negative bacteria. The lethal concentrations (LCs) of CA/CB1 on some typical Gram-negative bacteria are shown in Table 1. In general, the potencies of CB1 and that of CA on lysing Gram-negative bacteria such as *Klebsiella pneumoniae*, *Escherichia coli* and *Pseudomonas aeruginosa* are similar. The differences in LCs between CB1 and CA range only from 3% (*P. aeruginosa*) to 15% (*K. pneumoniae*). In contrast, for leukemia cells, the potency of CB1 and that of CA are significantly different, the IC_{50} values of CA are about two- to seven-fold the IC_{50} values of CB1. For example, the IC_{50} of CB1 is only 2.4 μM for Jurkat (E6-1) cancer cells but the IC_{50} of CA is 15.8 μM for the same cells. The different values of IC_{50} of CB1 and CA obtained from different leukemia cells, as shown in Table 1, may be caused by these cells, which were obtained from leukemia patients of different ages, sexes and races, with different growth rates and life cycles [2]. The fact that CB1 has a greater ability to kill leukemia cells than CA may be due to the difference in the sequence or to their three-dimensional structure. To further understand the correlation between cell killing ability and the peptide structure, the solution structure of CB1 was investigated by CD and NMR methods as shown below.

3.2. Secondary structure of CB1

CD spectra of CB1 without (dashed line) and with (solid line) 20% HFP (v/v) are shown in Fig. 1. Without the addition of HFP, CB1 shows negligible traces of secondary structure as shown by the negative minimum at around 200 nm. This implies that CB1 is in a random coil form in aqueous solution. In contrast, with the addition of HFP providing a membrane-like environment in the solution, about 55% of α-helix is

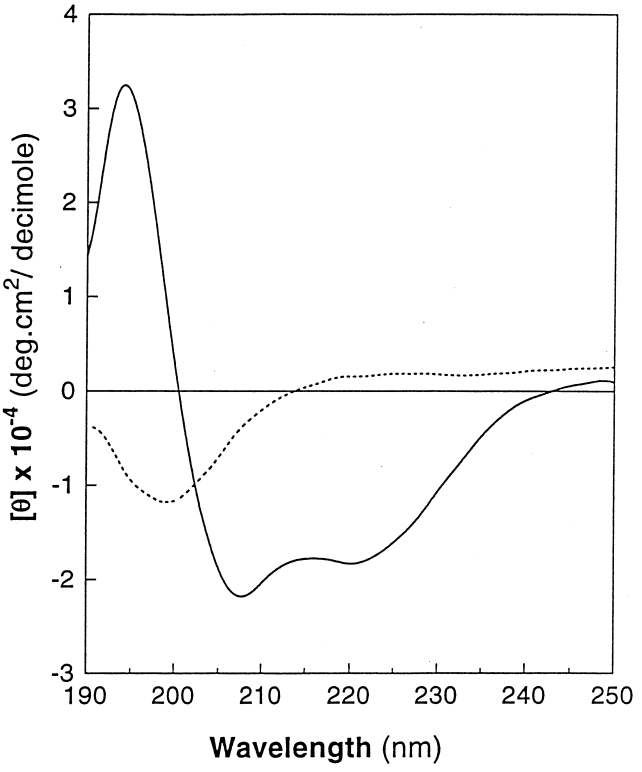

Fig. 1. CD spectra of CB1 with (solid line) and without (dashed line) 20% HFP (v/v).

Table 2
^{1}H chemical shifts (ppm) of CB1 in 20% HFP at pH 4.2 and 32°C

Residue	NH	CαH	CβH	CγH	Others
Trp-2		4.81	3.41		2H 7.38; 5H 7.15; 7H 7.53; 4H 7.28; 6H 7.53; NH 9.85
Lys-3	8.21	4.11	2.31, 2.37	1.35	δCH_2 1.77
Val-4	7.21	3.76	1.77	0.90, 0.80	
Phe-5	7.42	4.46	3.33, 3.17		2,6H 7.30; 3,5H 7.40, 4H 7.
Lys-6	7.97	4.18	2.02, 1.93	1.62	δCH_2 1.80; εCH_2 3.04
Lys-7	7.69	4.10	2.04	1.59, 1.48	δCH_2 1.74; εCH_2 3.03
Ile-8	7.94	3.81	2.04	1.75, 1.22	$\gamma CH_3$0.98; δCH_3 0.88
Glu-9	8.27	4.01	2.15	2.48, 2.28	
Lys-10	7.83	4.06	2.06, 1.87	1.52	δCH_2 1.71
Met-11	8.34	4.34	2.28	2.75, 2.66	δCH_3 2.05
Gly-12	8.83	3.90			
Arg-13	8.10	4.09	2.04, 1.94	1.72	δCH_2 3.27; δNH 7.36
Asn-14	8.04	4.58	3.16, 2.87	δNH_2 36.78, 7.13	
Ile-15	8.45	3.85	1.99	1.20, 1.81	$\gamma CH_3$0.97; δCH_3 0.90
Arg-16	8.19	3.99	1.97, 1.90	1.65	δCH_2 3.19; δNH 7.02
Asn-17	8.11	4.49	3.02, 2.84		δNH_2 7.56, 6.70
Gly-18	8.04	3.87			
Ile-19	8.16	3.74	1.94	1.65	$\gamma CH_3$0.87; δCH_3 0.80
Val-20	8.03	3.79	2.23	1.12, 1.00	
Lys-21	7.90	4.15	1.95	1.61	$\delta CH_2$1.71; $\varepsilon CH_2$3.01
Ala-22	7.93	4.36	1.56		
Gly-23	8.04	4.03, 4.25			
Pro-24	4.39	2.25, 2.05	1.83		$\delta CH_2$3.81, 3.68
Lys-25	7.83	4.06	2.06, 1.87	1.52	$\delta CH_2$1.71
Trp-26	7.65	4.49	3.43		2H 7.31; 5H 7.07; 7H 7.48; 4H 7.54; 6H 7.23; NH 9.57
Lys-27	7.45	3.91	1.81, 1.69	1.26	$\delta CH_2$1.33; $\varepsilon CH_2$3.00
Val-28	7.49	3.71	2.08	0.98, 0.88	
Phe-29	7.93	4.46	3.23, 3.18		2,6H 7.16; 3,5H 7.27; 4H 7.28
Lys-30	8.01	4.06	1.99	1.82	δCH_2 1.89
Lys-31	7.76	4.18	1.89, 1.81	1.45	δCH_2 1.75; εCH_2 3.04
Ile-32	8.01	3.94	1.99	1.68, 1.24	$\gamma CH_3$0.94; δCH_3 0.86
Glu-33	8.01	4.11	2.07, 2.00	2.37, 2.32	
Lys-34	7.83	4.30	1.97	1.59	δCH_2 1.77; εCH_2 3.08

All proton chemical shifts were measured with an error of ±0.02 ppm relative to sodium d_4-TSP. A single entry for a methylene group chemical shift indicates the two protons either overlap or are not unambiguously assigned.

induced as evidenced by the 208 and 222 nm negative minimum bands. The CD evidence of CB1 possessing the secondary structure in the HFP solution was clarified. This result may be a useful reference for the investigation of CB1 solution structure by using NMR techniques as shown below.

3.3. NMR experiments and analysis

Initially, one-dimensional ^{1}H NMR experiments were carried out at various temperatures and pHs to optimize the conditions for acquiring 2D NMR data. The results obtained from 1D NMR show that a pH value of 4.2 and a temperature of 32°C are optimal for conducting 2D NMR experiments. All the amino acid spin systems except for the first residue (Lys-1) were completely identified in the TOCSY spectrum. Sequence specific resonance assignment was carried out using standard procedures [29] and it was accomplished without much difficulty, due to the appreciable dispersion of the resonances of CB1 in 20% HFP and 32°C. The ^{1}H NMR resonance assignments of CB1 are presented in Table 2. Proline present at position 24 has a *trans* configura-

tion as indicated by the strong NOE cross peak between the α-protons of Gly-23 and the δ-protons of Pro-24. Helical segments are characterized by a weak $d_{\alpha N}(i,i+1)$ cross peak and strong $d_{NN}(i,i+1)$ connectivities. Fig. 2A shows the NH-αH region of the NOESY spectrum of CB1. The $d_{\alpha N}(i,i+1)$ connectivities are indicated for the two stretches from residues 4–17 and 29–34 (Fig. 2A). A series of sequential

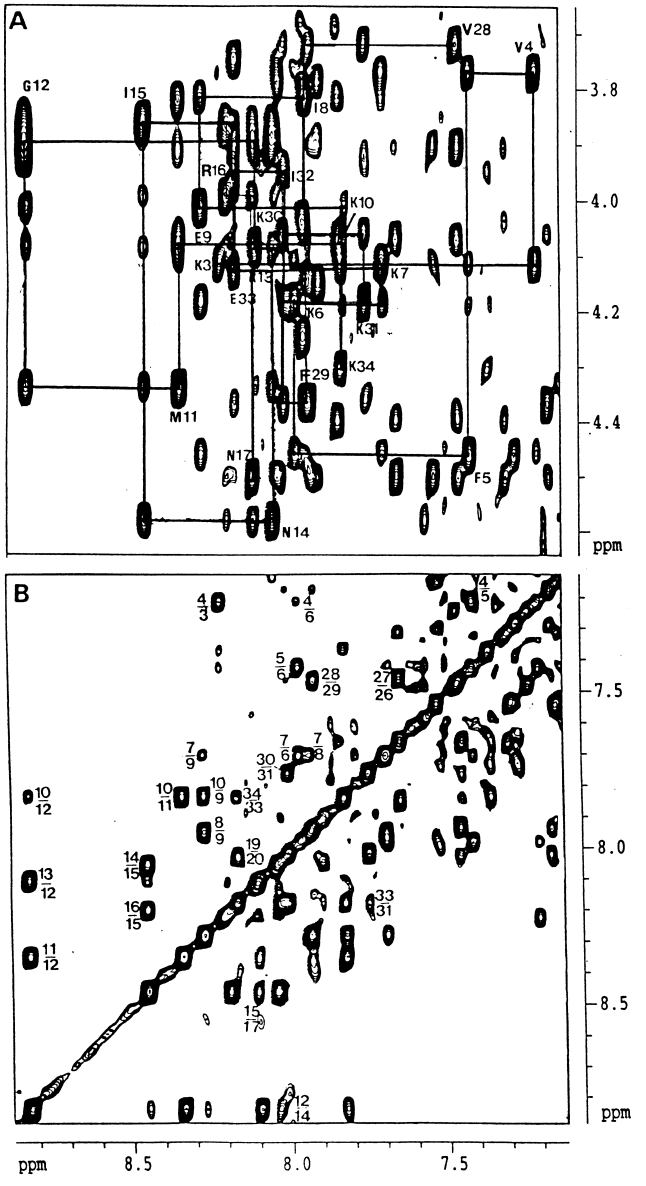

Fig. 2. Portion of the NOESY spectrum of CB1 in 20% HFP at a mixing time of 200 ms showing (A) NH-αH connectivities from residues 3 to 17 and 29 to 34 and (B) the amide region with $d_{NN}(i,i+1)$ and $d_{NN}(i,i+2)$ NOEs characteristic of a helical conformation.

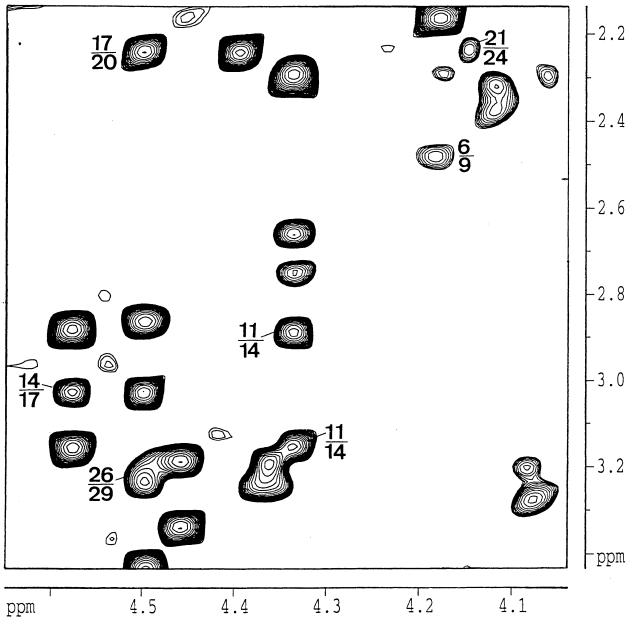

Fig. 3. Representative $d_{\alpha\beta}(i,i+3)$ NOE interaction from the same NOESY spectrum as in Fig. 2.

$d_{NN}(i,i+1)$ connectivities are observed throughout the entire sequence including a few $d_{NN}(i,i+2)$ NOEs (Fig. 2B). Together with the strong $d_{NN}(i,i+1)$ connectivities, helical segments show medium-range $d_{\alpha N}(i,i+3)$, $d_{\alpha N}(i,i+4)$ and $d_{\alpha\beta}(i,i+3)$ NOE interaction. Fig. 3 shows some of the representative $d_{\alpha\beta}(i,i+3)$ NOEs which are characteristic of helical conformation. Summaries of the sequential and medium-range NOEs observed for CB1 in 20% HFP are depicted in Fig. 4. In Fig. 4, several ambiguous NOEs were observed due to spectral overlap. About 17 of 43 such medium-range NOEs could be confirmed by carefully analyzing those peak shapes across the diagonal. These NOEs were used in the structure calculations. However, the obvious convergence of the structure is not only based on these NOEs but is rather due to the whole set of 350 unambiguous NOEs. The bent angle between two helices is quite converged due to NOEs of side chains within the bent regions from positions 19 to 26. These medium-range NOEs obtained from the bent region of CB1 are: $27\delta_{CH2}$#/24αH, 24γH#/26HN, 22βH#/26HN, 24αH/26εNH, 21αH/26εNH, 24γH#/26εNH, $19\delta_{CH3}$#/26εNH, 24αH/26δH and 23αH/26δH. Some representative NOEs are shown in Fig. 5. Several NOEs are obtained from the side chain of Trp-26. The indole proton of Trp-26 has a NOE

Fig. 4. Schematic representation of the NOEs observed for CB1 in 20% HFP. NOE intensities are indicated by the thickness of the bars. NOEs that are obscured because of overlapping resonance are indicated by dotted lines.

coupling with δ_{CH3} of Ile-19 to α-protons of Lys-21 and Pro-24. These NOEs are partially used to determine the bent angle formed between two α-helices. The NOE pattern identifies two helical segments spanning residues 3–22 and 26–33. Deviations from the reference random coil values for the α-proton chemical shifts can give valuable information on the conformational status of a peptide or protein [30]. When both α-proton chemical shifts of CA [14] and CB1 (present work, data not shown) are compared, we observe that CA possesses slightly higher helical content than CB1. This implies that the strength of the secondary structure of peptides may not be essential for a better cell killing ability since the potency of CA in cancer cells is less than that of CB1 (see Table 1).

3.4. Structure calculation

A total of 350 distance constraints including intra-residue, sequential and medium-range constraints derived from the NOESY spectrum of CB1 were classified into four different distance ranges [14]. Pseudo atom corrections were used for methylene and methyl protons [29]. The three-dimensional structure calculation of CB1 is based on the application of a dynamical simulated annealing protocol [25,26]. Briefly, the simulated annealing protocol consisted of 20 ps of high-temperature molecular dynamics

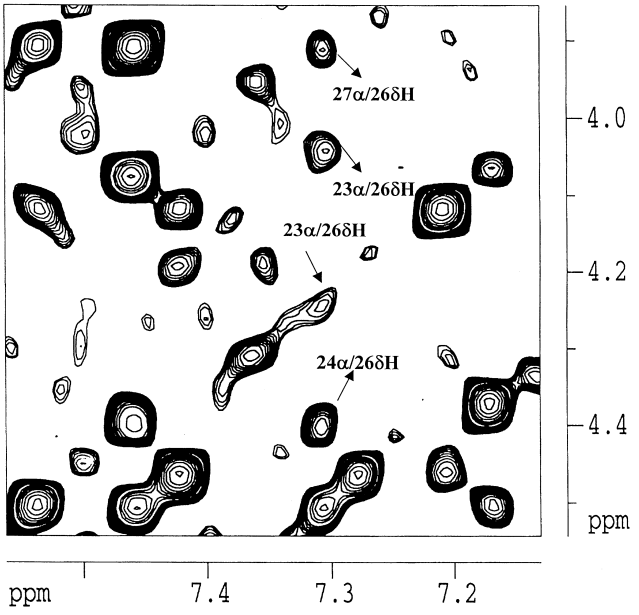

Fig. 5. A representative spectrum showing some significant NOEs, which partially define the bent angle of CB1.

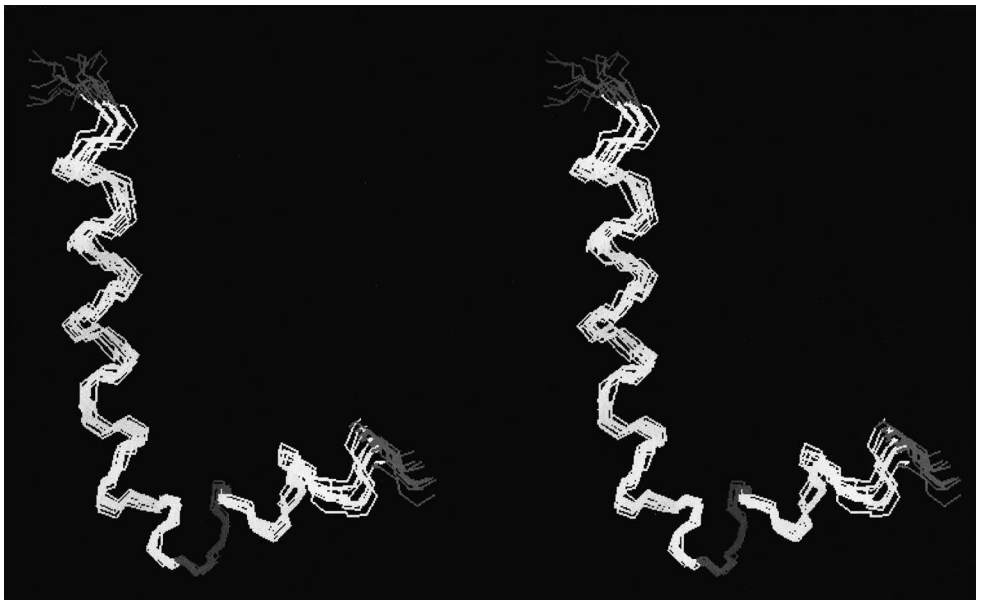

Fig. 6. Stereo view of CB1 showing the backbone superimposition of the 12 final simulated annealing structures. Vertical and horizontal secondary structures represent N- and C-terminal α-helices, respectively.

with a low weighting on the NOE constraints at 1000 K followed by 10 ps of dynamics with an increased weighting on the NOE constraints. The system was then cooled to 100 K over 15 ps and the structures were subjected to 200 cycles of energy minimization. A series of template structures with randomized coordinates were used to generate a set of 50 simulated annealing structures. The structures were further refined by restraint Powell energy minimization (steepest descent 50 steps and Powell 100 steps), which was based on the CHARMM program (Charm version 23.2) [31]. Among 50 simulated annealing structures, 12 structures were selected based on the minimum NOE violation and the lowest conformational energy. Fig. 6 shows the superimposition of the backbone atoms of CB1 for the 12 refined structures. The statistics of the final CB1 structure are as follows: (i) energy: 426.9 kcal/mol for the total energy after minimization, 44.8 kcal/mol for the bond energy, 418.9 kcal/mol for the angle energy, 190.6 kcal/mol for the dihedral energy, 17.6 kcal/mol for the improper energy, −13.5 kcal/mol for the Leannard Jones energy and −231.6 kcal/mol for the electrostatic energy. (ii) RMSD: 1.33 Å for the heavy atoms, 0.62 Å for the backbone and 0.45 Å for the structural region. Based on the results, CB1 was found to have a bent angle ranging from 100 to 110° and helical motif of N-terminal α-helix from positions 3 to 22 and C-terminal α-helix from positions 26 to 33. An analysis of the ϕ–ψ combinations for the averaged structure of CB1 shows that residues 3–22 and 26–34 are well defined in the α-helical region of the Ramachandran plot as shown in Fig. 7. Three amino acids, namely Gly-23, Pro-24 and Trp-2, are not in the allowed region of the Ramachandran plot. This also supports the NOE data obtained for the length of the helical segments spanning residues 3–22 and 26–34. Lys-25 is partially incorporated in the hinge region along with Gly-23 and Pro-24. However, this residue was also found in the α-helical region (see Fig. 7). Based on the defined NMR structure of CB1, the helical wheel projections [32] for N-terminal and C-terminal α-helices are shown in Fig. 8A,B, respectively. The wheels indicate that CB1 possesses two amphipathic α-helices.

3.5. Biological implications

Based on our experimental observations for membrane lysis induced by CB and its analogs CB1 and cecropin B3 (CB3), by using encapsulated-dye leakage [20] and electron spin resonance [33], the strengths of lytic activity of these custom peptides on lipid bilayers may depend not only on the char-

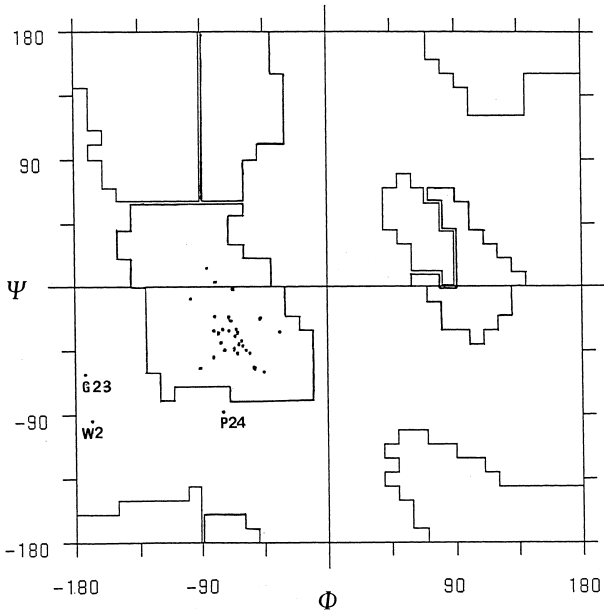

Fig. 7. Ramachandran plot of backbone conformational angles (ϕ–ψ) for the averaged simulated annealing structures.

acteristics of α-helix but also on the orientation of the peptide upon approaching the surface of polar head lipids. Regarding the latter factor, orientation of the peptide, we believe that the bent angle of the peptide may be one of the key factors to determine the orientation when the peptide's environment is transferred from an aqueous solution (peptide with random coil) to a polar milieu (peptide with two α-helices). Under the conditions of the existing secondary motif with a bent angle between two helices, peptides thus perform their membrane lysis activity. A preliminary study on the correlation between the bent angle of CB1 in the polar HFP environment and the peptide's biological activity was therefore carried out and the results are shown in this communication. The NMR structures (in HFP) for CB and CB3 are under investigation. The NMR structures in HFP of these peptides can be the basis for our future peptide NMR studies in the cell membrane system.

As observed from the reported NMR structures of certain members of the cecropin family like cecropin A [14] and cecropin P1 [18], all the peptides form secondary structures in the membrane-like environment. In the present study, a custom designed peptide, cecropin B1, was also found to have a secondary structure in HFP solution. The formation of the secondary structure, therefore, may be a prerequisite for the lytic property of the peptide. Once the condition for forming the secondary structure is satisfied, the characteristics of the α-helix may appear to be an influential factor in determining the potency of the peptide on membrane lysis. For example, a custom peptide, CB3, with two hydrophobic α-helical segments does form a secondary conformation in HFP solution or cell membranes; however, it lacks the ability to lyse either bacteria or cancer cells [34]. For cecropin peptides, this implies that an amphipathic α-helix is necessary for performing valid cell killing activity. The role of the hydrophobic α-helix in the peptide may not be significant on lysing cell membrane. For instance, CB1, having two amphi-

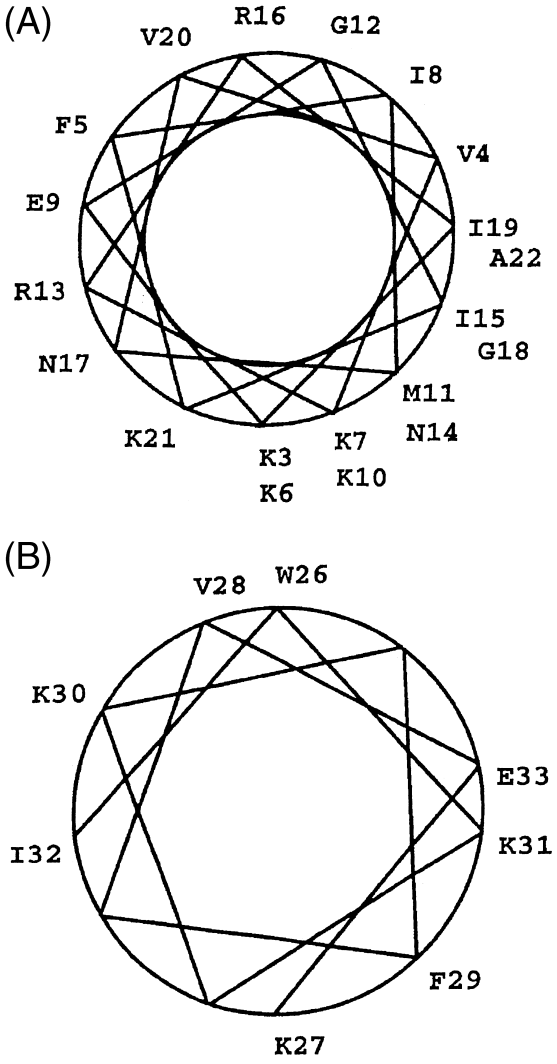

Fig. 8. Helical wheel projection of CB1 (A) N-terminus amphiphilic helix and (B) C-terminus amphiphilic helix.

pathic α-helices, has a similar ability to kill bacteria as CA, which has one amphipathic and one hydrophobic α-helix (see Table 1). Moreover, CB1 has a much greater ability to lyse cancer cells than CA does (see Table 1). This may imply that a peptide with two hydrophilic α-helices is in a better position to kill transformed eukaryotic cells than a peptide with one hydrophilic and one hydrophobic helix.

Based on the above observations of the biological activities of CB1 on bacteria and cancer cells, in this communication we further investigate the structure of CB1 by CD and search for more details by the NMR technique. The results confirm that CB1 possesses secondary structure with the helices from residues 3–22 (N-terminal α-helix) and 26–34 (C-terminal α-helix; see Fig. 7). The hinge region between the N-terminal and C-terminal α-helices is partially incorporated into the region together with a pair of residues, Gly-23 and Pro-24. With consideration of the optimal conditions used for CA [14] and CB1, the difference between the two peptide structures lies with the bent angle between two helices. CA has a wider flexibility with an angle from 70 to 100° and CB1 has a more compact form with the angle extending from 100 to 110°. The narrower flexibility of the bent angle for CB1 may be one of the factors leading to the peptide's higher membrane lysis ability on cancer cells since the structural flexibility of the peptide may determine the insertion efficiency at the early stage of membrane lysis. Although other factors such as the self-orientation and the stability of the helix in peptides may also play a role in the efficiency of lysing cell membranes, studies on CA [14] and CB1 cannot clearly identify these two factors under the investigations of the current NMR spectroscopy in HFP solutions. In addition, the characteristics of α-helix may play a role in lysing cells. For example, our designed peptide, CB3, having two hydrophobic α-helical segments, shows a different degree of lysis ability on lipid bilayers of different compositions as compared with CB1 [20].

In summary, the solution structure of a custom antibacterial peptide, CB1, with a higher leukemia cells killing potency than the natural peptide, CA, was determined. This custom designed peptide with an α-helical structure in the membrane-like environment is similar to the reported natural CA and has the ability to lyse bacteria [2]. The differences in cell killing ability between CB1 and CA may be due to the peptides' differences in bent flexibility and other factors such as helical self-orientation and stability. The net charges and characteristics of the α-helix may also influence the structural construction. To obtain information regarding the peptide orientation and stability, an NMR study involving micelles in peptide solution will be conducted in the future.

Acknowledgements

This work was supported in part by Grant HKUST 6192/99M from Research Grant Council of Hong Kong and in part by Grants NSC 88-2113-M007-028 and NSC 88-2311-B007-021 from the National Science Council of Taiwan (C.Y.).

References

[1] R.E.W. Hancock, R. Lehrer, Trends Biotechnol. 16 (1998) 82–88.
[2] H.M. Chen, W. Wang, D. Smith, S.C. Chan, Biochim. Biophys. Acta 1336 (1997) 171–179.
[3] H.G. Boman, Annu. Rev. Immunol. 13 (1995) 61–92.
[4] R.A. Cruciani, J.L. Barker, M. Zasloff, H.C. Chen, O. Cloamonici, Proc. Natl. Acad. Sci. USA 88 (1991) 3792–3796.
[5] A.J. Moore, D.A. Devine, M.C. Bibby, Peptide Res. 7 (1994) 265–269.
[6] D. Winder, W.H. Gunzburg, V. Erfle, B. Salmons, Res. Commun. 242 (1998) 608–612.
[7] J. Kim, M. Mosior, L.A. Chung, H. Wu, S. McLaughlin, Biophys. J. 60 (1991) 135–148.
[8] N. Ben-Tal, B. Honig, Biophys. J. 71 (1997) 3046–3050.
[9] K. Hristova, M.E. Selsted, S.H. White, J. Biol. Chem. 272 (1997) 24224–24233.
[10] R.E.W. Hancock, Lancet 349 (1997) 418–422.
[11] D. Hultmark, H. Steiner, T. Rasmuson, H.G. Boman, Eur. J. Biochem. 106 (1980) 7–16.
[12] H. Steiner, D. Hultmark, A. Engstrom, H. Bennich, R. Kaput, H.G. Boman, Nature 292 (1981) 246–248.
[13] H.G. Boman, D. Hultmark, Annu. Rev. Microbiol. 41 (1987) 103–126.
[14] T.A. Holak, A. Engstrom, P.J. Kraulis, G. Lindeberg, H. Bennich, T.A. Jones, A.M. Gronenborn, G.M. Clore, Biochemistry 27 (1988) 7620–7629.
[15] H.G. Boman, D. Wade, I.A. Boman, B. Wahlin, R.B. Merrifield, FEBS Lett. 259 (1989) 103–106.
[16] D. Sipos, K. Chandrasekhar, K. Arvidsson, A. Engstrom, A. Ethenberg, Eur. J. Biochem. 199 (1992) 285–291.

[17] J.-Y. Lee, A. Boman, C. Sun, M. Andersson, H. Jornvall, V. Mutt, H. Boman, Proc. Natl. Acad. Sci. USA 86 (1989) 9159–9162.
[18] D. Sipos, M. Andersson, A. Ehrenberg, Eur. J. Biochem. 209 (1992) 163–169.
[19] W. Xia, Q. Liu, J. Wu, Y. Xia, Y. Shi, X. Qu, Biochim. Biophys. Acta 1384 (1998) 299–305.
[20] W. Wang, D.K. Smith, K. Moulding, H.M. Chen, J. Biol. Chem. 273 (1998) 27438–27448.
[21] S.-C. Chan, L. Hui, H.M. Chen, Anticancer Res. 18 (1998) 4467–4474.
[22] A. Bax, D.G. Davis, J. Magn. Reson. 65 (1985) 355–360.
[23] C. Griesinger, G. Otting, K. Wuthrich, R.R. Ernst, J. Am. Chem. Soc. 110 (1998) 7870–7872.
[24] D. Marion, K. Wuthrich, Biochem. Biophys. Res. Commun. 113 (1983) 967–974.
[25] M. Nilges, G.M. Clore, A.M. Gronenborn, FEBS Lett. 229 (1988) 317–324.
[26] M. Nilges, A.M. Gronenborn, A.T. Brunger, G.M. Clore, Protein Eng. 2 (1988) 27–38.
[27] A.T. Brunger, J. Kuryan, M. Karplus, Science 235 (1987) 458–460.
[28] A.T. Brunger, G.M. Clore, A.M. Gronenborn, M. Karplus, Protein Eng. 1 (1987) 399–406.
[29] K. Wuthrich, NMR of Proteins and Nucleic Acids, John Wiley and Sons, New York, 1986, pp. 130–161.
[30] D.S. Wishart, B.D. Sykes, F.M. Richards, J. Mol. Biol. 222 (1991) 311–333.
[31] B.R. Brooks, R.E. Brucoleri, B.D. Olafson, D.J. States, S. Swaminathan, M. Karplus, J. Comput. Chem. 4 (1983) 187–217.
[32] M. Schiffer, A.B. Edmundson, Biophys. J. 7 (1967) 121–135.
[33] S.-C. Hung, W. Wang, S.I. Chan, H.M. Chen, Biophys. J. 77 (1999) 3120–3133.
[34] S.C. Chan, W.L. Yau, W. Wang, D.K. Smith, F.S. Sheu, H.M. Chen, J. Peptide Sci. 4 (1998) 413–425.